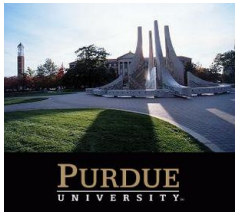

Modeling of Macroscopic Melt Layer Splashing during Plasma Instabilities

Gennady V. Miloshevsky and Ahmed Hassanein

School of Nuclear Engineering, Purdue University, West Lafayette, IN, USA

Abstract

Damage of plasma-facing components in tokamaks due to various plasma instabilities remains one of the most important problems in their successful operation. Macroscopic melt losses from divertor plates and nearby components into core plasma are significant material erosion lifetime and plasma contamination issues. The classical linear stability analysis and computational modeling are used to predict the onset and growth of surface waves on the plasma-liquid interface. The whole course of development, growth, and breakup of waves at the plasma-liquid metal interface is modeled for the first time. The new physics mechanism and underlying processes involved in breakdown and erosion of a thin liquid metal layer are presented. It is found that the melt layer undergoes macroscopic motion, bulk melt splitting, development and growth of liquid tungsten ligaments that transform to thin threads and eventually break into droplets. These results shed light on the physical behavior of a melt layer under transient plasma instabilities such as edge-localized modes and disruptions.

1. Introduction

Transient heat loads due to plasma disruptions (20-100 MJ/m2) and edge-localized modes (ELMs, ~1-3 MJ/m2) can erode divertor materials in tokamak devices [1]. The deposited high-heat power can generate vapor clouds, melt plasma-facing materials, cause ejection of droplets, with subsequent surface damage and cause serious plasma contamination [2]. One of the most significant problems during plasma instabilities is the macroscopic melt losses from a metallic divertor plate and potential contamination of the core plasma. Melt layer splashing due to macroscopic melt motion was investigated in a number of laboratory experiments carried out using laser, electron and plasma accelerator devices with different heat loads and time durations [3]. The plasma impact momentum and/or Lorentz force were found to be responsible for macroscopic melt splashing.

The behavior of melt layer under plasma disruptions is not well-understood. Description and quantification of physical mechanisms and processes governing melt layer motion and macroscopic losses during the course of plasma disruptions and ELMs are important for development of fusion reactors. Melt layer motion and macroscopic losses are mainly driven by ablation physics of ejected material, and less by evaporation/ionization physics. The development of Kelvin-Helmholtz (K-H) instability at the plasma-melt interface could be one of mechanisms for the macroscopic loss of a melt layer [4]. The high-speed plasma flowing along a melted layer can produce surface melt perturbations and growth of waves. Breakup of surface waves can later result in liquid droplet formation and these macroscopic droplets can be splash into the plasma. The theoretical studies and modeling of momentum transfer from the impacting plasma or other volumetric force (Lorentz force) to a melt layer are very important for understanding the physical mechanisms involved in splashing and droplet formation.

2. Theoretical and Computational Models

2.1. Linear Stability Theory of Plasma-Liquid Metal Flows

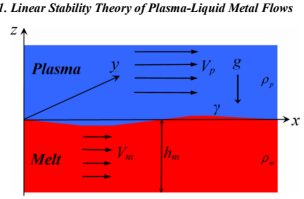

Fig. 1. Sketch of the parallel flow of plasma and melt streaming respectively with velocity V_p and V_m, of densities ρ_p and ρ_m, and of interfacial tension γ. Gravity acts in the negative z-direction. h_m is the melt depth.

- plasma-tungsten melt parameters:

$V_p \sim 10^6$-10^7 cm/s; $\rho_p \sim 10^{-10}$-10^{-9} g/cm^3

$V_m \sim 10^2$ cm/s; $\rho_m \sim 17.6$ g/cm^3

$\gamma \sim 2500$ dyn/cm; $g \sim 981$ cm/s^2

$h_m \leq 400$ μm

- the linear stability analysis given in a textbook of Chandrasekhar [5, p. 481] for inviscid and infinitely thick fluids is applied to the plasma-liquid metal system with extension to account for a finite thickness, h_m, of a melt layer
- the dispersion relation [5,6]:

$$n = -k_x\left(\frac{\rho_m V_m + \rho_p V_p}{\rho_m + \rho_p}\right) \pm \left[\left(g\kappa\frac{\rho_m - \rho_p}{\rho_m + \rho_p} + \frac{\kappa^3\gamma}{\rho_m + \rho_p}\right)\tanh(\kappa h_m) - \frac{k_x^2\rho_m\rho_p}{(\rho_m + \rho_p)^2}(V_m - V_p)^2\right]^{1/2}$$

phase velocity of waves; stabilizing gravity for long waves; stabilizing tension for short waves; destabilizing inertia

$\kappa = \sqrt{k_x^2 + k_y^2} = 2\pi/\lambda$ - real wave number associated with small disturbances $\sim\exp(i(k_x x + k_y y + nt))$

λ - wavelength; k_x and k_y - x and y components of wavenumber κ; n - frequency

$$\textbf{Instability} \rightarrow \frac{\kappa^2\rho_m\rho_p}{(\rho_m + \rho_p)^2}(V_m - V_p)^2 > \left(g\kappa\frac{\rho_m - \rho_p}{\rho_m + \rho_p} + \frac{\kappa^3\gamma}{\rho_m + \rho_p}\right)\tanh(\kappa h_m)$$

- the maximum velocity difference required to generate the K-H instability:

$$\Delta V = |V_m - V_p| > \sqrt{\frac{\rho_m + \rho_p}{\rho_m\rho_p}\left(\frac{G}{\kappa} + \gamma\kappa\right)\tanh(\kappa h_m)}$$ with $G = g(\rho_m - \rho_p)$ - gravitational restoring force

2.2. Computational Model of Two-Fluid Plasma-Liquid Metal Flows

- plasma and tungsten melt are treated as two incompressible, inviscid, and immiscible fluids of different densities separated by a sharp interface
- volume of fluid model [7] is used to describe plasma and melt as two pure fluids with volume fractions of plasma α_p and liquid metal α_m near the interface (α_p+α_m=1), while away from the interface the flow contains only one fluid
- single-field velocity and pressure are used for liquid metal and plasma; velocity is assumed to be continuous at the interface, but the pressure undergoes a jump due to the surface tension
- volume fraction of plasma is calculated solving the continuity equation

$$\frac{\partial\alpha_p}{\partial t} + \nabla\cdot(\alpha_p\mathbf{V}) = 0$$ with $\mathbf{V} = (V_x, V_z)^T$ - the single velocity field and α_m=1- α_p

- single momentum equation is solved

$$\rho\frac{\partial\mathbf{V}}{\partial t} = -\nabla p + \mathbf{F}_\sigma + \rho\mathbf{g}$$ with p - the single field pressure; $\mathbf{F}_\sigma$ – surface tension force and $\rho = \alpha_p\rho_p + \alpha_m\rho_m$

- the energy equation is not solved assuming that vaporization of tungsten at the plasma-liquid interface is negligible and the thermal energy is not exchanged between the fluids
- the system of above two-fluid equations is solved using finite volume discretization schemes implemented in the commercial FLUENT program package [8]

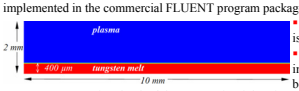

Fig. 2. Representative sketch of the computational domain used in simulations of two-fluid plasma-liquid tungsten flows. Liquid tungsten is shown in red and plasma is displayed in blue.

- mesh with 400x80 cells (step size 25 μm) is used
- periodic boundary conditions are applied in flow direction; top and bottom domain boundaries are modeled as frictionless walls
- all simulations are done for plasma and melt velocities 10^7 cm/s and 10^2 cm/s, respectively; plasma density is 10^{-9} g/cm^3
- volume fractions and densities of two fluids are implemented in the C code as a user defined function in the FLUENT solver
- instability initiated by sinus disturbance of the two-fluid interface $\sim a\cdot\sin(2\pi x/\lambda)$ with small amplitude a and wavelength λ was implemented in the C code as a user defined function in the FLUENT solver
- surface disturbance within a wavelength range from 10 mm to 0.1 mm (1 to 100 wavelengths per the length of the computational domain) was investigated for nonlinear growth of waves

3. Analytical and Computational Results

3.1. The Onset of the K-H Instability from the Linear Theory

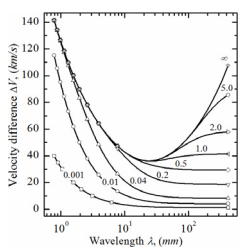

Fig. 3. Critical velocity difference as a function of wavelength, λ=2π/κ, for a tungsten melt layer of various thickness. Labels near curves indicate the depth of melt layer h_m in cm. The density of impacting plasma is 10^{-9} g/cm^3.

Case of infinitely deep melt layer:

- for $h_m \rightarrow \infty$, the dispersion curve is parabolic-like; unstable region is above this curve
- growing waves on a deep melt layer can be generated by the plasma stream with minimum velocity 3.6·10^6 cm/s; the most "dangerous", critical wavelength λ_c~24 mm
- waves with wavelengths much larger than λ_c are damped due to gravity effects (long waves on right-hand side of Fig. 3); waves with wavelengths much smaller than λ_c are suppressed due to surface tension effects (short waves on left-hand side of Fig. 3)

Case of melt layer with finite depth:

- as the melt depth h_m decreases, long-length waves become the most unstable ones; for $h_m \leq 0.5$ cm, disturbances with very long wavelengths are predicted as the most unstable waves
- critical velocity difference is decreased with a critical wavelength shifted toward long wavelengths; for $h_m < 100$ μm, left-hand side portions of dispersion curves (slopes) become more and more flat
- thin melt layers with h_m~10 μm can be disturbed in a wide range of wavelengths by the plasma stream with the critical velocity much smaller than that required for a thick melt layer
- *plasma density, surface tension and magnetic field effects on dispersion curves (results not shown):*
  - stream of more dense plasma along the melt surface causes more easy breakdown of a melt layer;
  - increase in surface tension has more stabilizing effect on waves with short wavelengths, while long wavelengths are not affected at all;
  - all disturbances are strongly suppressed by the magnetic surface tension with the magnetic field acting in the flow direction; magnetic field perpendicular to the flow direction has no influence on surface waves

3.2. Simulations of Plasma-Liquid Tungsten Flows

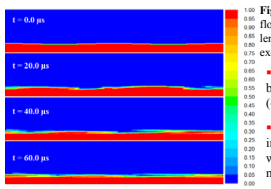

Fig. 4. Fields of volume fractions for plasma-liquid tungsten flow at different times. Two wavelengths with λ=5 mm per the length of the computational domain (10 mm) were initially excited at t=0.0 μs.

- melt is affected within a thin surface layer, while the bulk of metallic melt is not disrupted during long times (~60 μs)
- long waves with λ=5 mm do not grow as time increases; the same behavior was found for a wavelength with λ =10 mm; breakdown of the tungsten melt into liquid droplets is not observed for long waves

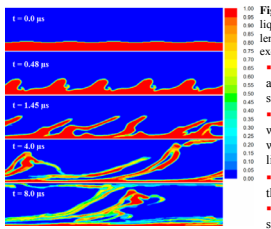

Fig. 5. Evolution in time of volume fraction fields for plasma-liquid tungsten flow. Five wavelengths with λ =2 mm per the length of the computational domain (10 mm) were initially excited at t=0.0 μs.

- at t=0.48 μs, liquid tungsten waves grow quickly in amplitude with development of small saw-tooth-like secondary instability fingers
- at t=1.45 μs, the plasma flow elongates liquid metal waves forming five localized protrusions (ligaments) with ligament's width smaller than their lengths; as ligaments lengthen, they become curved and thinner
- at t=4 μs, ligaments collide trapping small pockets of the plasma
- at t=8 μs, topological structures of tungsten patterns suspended in the plasma become highly irregular

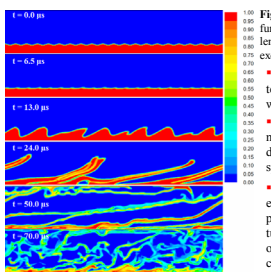

Fig. 6. Plasma-liquid tungsten volume fraction fields as a function of time. Twenty wavelengths with λ=0.5 mm per the length of the computational domain (10 mm) were initially excited at t=0.0 μs.

- at t=6.5 μs, wave crests are regularized by the surface tension strongly damping short-length waves; ripply wave structures without vortices are still remaining
- at t>10 μs, the most dangerous and fastest growing new waves with larger wavelengths within 1-2 mm self-develop; at t=13 μs, the growth of these melt waves splits the bulk of a melt layer
- at t=24 μs, liquid tungsten waves transform to elongated ligament protrusions penetrating into the plasma; ligament lengthening is supported by influx of tungsten from the bottom with their coalescence occurring due to collisions; bubbles of plasma become confined within a melt during ligament agglomerations
- at t=50 μs, narrow and long liquid tungsten threads are formed; plasma flow changes the shape of threads creating thinner and thinner segments; sufficiently large surface-tension force of tungsten liquid holds the thread's interface together for long times; thin threads are still bounded to the bottom
- at t=70 μs, liquid tungsten threads are highly thinned and eventually can break into droplets; size of droplets estimated from the diameter and length of ligaments within the range of ~25-200 μm

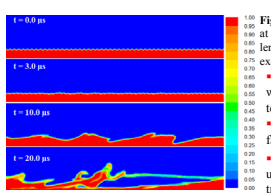

Fig. 7. Volume fraction fields of plasma-liquid tungsten flow at different times. Fifty wavelengths with λ=0.2 mm per the length of the computational domain (10 mm) were initially excited at t=0.0 μs.

- test case was ran until 20 μs to check if even smaller wavelengths are severely suppressed by the surface tension force
- these short wavelength corrugations are regularized faster at t=3.0 μs compared to previous simulation case
- at t=10 μs, four large waves are well developed and undergo localized growth with subsequent transformations into ligaments (t=20 μs)

Summary

- The focus of this work is on understanding the underlying physical processes involved in the breakdown and erosion mechanism of a liquid metal layer, macroscopic melt motion and losses during plasma disruptions in tokamaks. Linear stability analysis and computer simulations of the whole process of development, growth and breakup of waves at the plasma-liquid metal interface are presented for the first time. It is found that macroscopic motion and melt layer losses involve the onset of disturbances on the surface of a melt layer with relatively long wavelengths compared to the melt thickness, the formation of liquid tungsten ligaments at wave crests and their elongation by the plasma stream with splitting of the bulk of the melt, and the development of long, thin threads that eventually break into liquid droplets. These results advance the current understanding of the physics involved in the mechanism of melt layer breakdown and droplet generation processes.
- The inviscid stability analysis predicts that plasma streams with velocities of 10^6-10^7 cm/s can generate the growth of surface disturbances on a thin melt layer (≤400 μm) in a wide range of wavelengths. Short-length waves are strongly damped by the surface tension force. Long waves are predicted as the most unstable ones. However, numerical simulations demonstrated that long waves (5 and 10 mm) do not grow on the surface of a melt layer with the length of 10 mm and the depth of 400 μm. Understanding this issue will require further studies to reveal whether the finite dimensions of the computational domain may play a role in the suppression of long waves. It is found that the most dangerous waves correspond to ~1-2 mm (five-ten wavelengths). The surface disturbances with twenty and fifty wavelengths were initially regularized by the surface tension force. However, these short wavelength disturbances give rise to the growing of new waves with a critical wavelength on the order of 1-2 mm. These relatively long waves in comparison to the melt thickness (0.4 mm) undergo localized growth with transformations into long ligaments and threads that eventually can fragment into liquid droplets. The bulk of the melt layer initially splits and disintegrates into ligaments and further into liquid droplets. This mechanism of melt layer breakdown is completely different from that assuming the K-H instability is induced by the "plasma wind" on the surface of a liquid melt with droplets formed at peaks of surface waves and dragged away by the plasma flow. This classical picture of the K-H instability is not observed in our simulations. No surface waves which amplify to form a periodic array of compact spanwise rollers with conventional K-H finger-like projections that eventually break off to form droplets are revealed.
- The simulation results shed light on the physical mechanism of macroscopic melt losses that can lead to significant erosion of metal surfaces. It is predicted that about 80-90% of the melt layer thickness can be lost due to plasma impact in the form of liquid ligaments. This fraction may be overestimated because the adhesion force stabilizing liquid tungsten near the solid-melt interface was not included in the modeling. However, these data clearly indicate that plasma momentum affects the bulk of a melt layer leading to its macroscopic motion and considerable metal erosion.

References

1. G. Federici, Phys. Scr. T124 (2006) 1.
2. A. Hassanein, V. Belan, I. Konkashbaev, et al., J. Nucl. Mater. 241-243 (1997) 288.
3. G. Federici, A. Zhitlukhin, N. Arkhipov, et al., J. Nucl. Mater. 337-339 (2005) 684.
4. B. Bazylev, G. Janeschitz, I. Landman, et al., Phys. Scr. T128 (2007) 229.
5. S. Chandrasekhar, Hydrodynamic and Hydromagnetic Stability, Oxford University, London, 1961, p. 481.
6. Y. Bartosiewicz, J. Laviéville, J.-M. Seynhaeve, Int. J. Heat Fluid Flow 29 (2008) 460.
7. C. W. Hirt, B. D. Nichols, J. Comput. Phys. 39 (1981) 201.
8. Fluent-6.3 2006 *User's Guide* Fluent Inc.

Acknowledgement

This work is supported by the U.S. Department of Energy, Office of Fusion Energy Sciences. TeraGrid computational resources provided by the NCSA under grant TG-PHY090096. The authors acknowledge the NCSA for providing FLUENT software.